Drainage induced convection rolls in foams I:

Convective bubble motion in a tilted tube

S.J. Cox[a], M.D. Alonso, D. Weaire and S. Hutzler

School of Physics, Trinity College, Dublin 2, Ireland

Abstract. When liquid is added to a foam at sufficiently large flow rates, convective bubble motion will occur. Experiments are described in which the foam is confined in a tube which is tilted from the vertical. The theory of foam drainage is applied to this problem to show that the critical angle of tilt θ_c at which convection occurs is related to the liquid flow-rate Q by $\theta_c \propto Q^{-3/4}$.

PACS. 82.70.Rr Aerosols and Foams – 83.60.Wc Flow instabilities

1 Introduction

In the physics of liquid foams, drainage (the passage of liquid through the foam in response to gravity or pressure gradients) plays a central role [1]. If an aqueous foam is freshly created, it typically takes a few minutes to come into equilibrium under gravity. During this period drainage adjusts the vertical profile of the liquid fraction. If the foam is fed at the top with a supply of liquid, this may be called forced drainage. If the imposed flow rate is constant the result is steady drainage. Unless the flow rate is very small, the liquid fraction is approximately constant over most of the foam column, offering a very simple system for experiment and analysis, both of which have been pursued extensively in recent years [2, 3]. There is a good overall understanding of steady drainage, based largely on such experiments. Only the finer details of the microscopic flow that underlies our semi-empirical theories require to be interpreted [4].

When steady drainage experiments were pursued to high flow rates (and hence high liquid fraction) a new phenomenon emerged. The uniform flow, in which the foam structure remained fixed, was replaced by one in which there was a convective motion of the bubbles [5, 6, 7].

For a typical polydisperse foam, the convective motion progressively deposits the smaller bubbles at the bottom of the column, establishing a vertical gradient of bubble size, which in

---

[a] *Present address: Institute of Mathematical and Physical Sciences, University of Wales Aberystwyth, SY23 3BZ, UK. Email: foams@aber.ac.uk*

turn suppresses the motion [8]. For a monodisperse foam, the convective motion continues indefinitely, so this is the usual objective of study in attempts to understand convection.

In the present paper we present a variation of the now familiar experiment: the column is tilted away from the vertical. With such a tilt, convection is observed even at quite small flow rates. We are able to account for the convection in this case in terms of a simple theory in which it is seen to be driven by the transverse variation (across the column) of liquid density, in equilibrium.

This limited success may offer insight and confidence that the spontaneous convective instability in a vertical column can be adequately explained in similar terms. We shall return to that objective in a further paper.

The behaviour of the draining tilted foam is reminiscent of the Boycott effect [9], which describes how the sedimentation of particles suspended in a fluid is faster in a tilted tube than in a vertical one. The explanation of this phenomenon [10] is that in the vertical tube the particles have to move against the static fluid. When the tube is tilted, the concentration of particles below the axis of the tube grows and the fluid rises above the axis. The convection produced helps the particles to sediment faster. An analogous situation has been found in granular materials where the flow of grains out of a tube is fastest at angles between $30°$ and $45°$ degrees from the vertical [11].

However, although close analogies have been found in many aspects of the behaviour of foams and granular materials, it is important to stress that there is no trivial relationship between them.
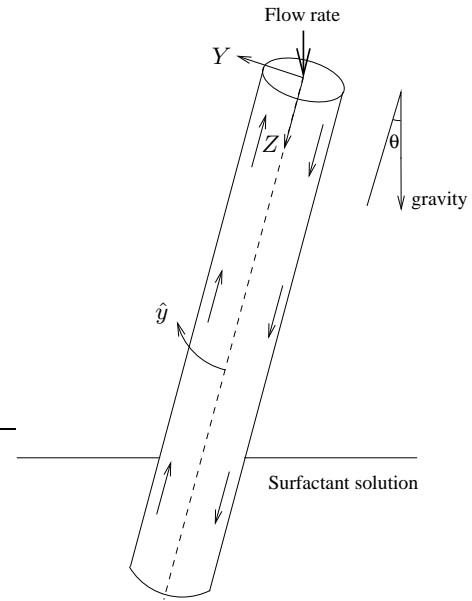

Fig. 1. A sketch of the convective roll in a tilted tube, showing the (Y, Z) coordinate system used in the analysis and the $\hat{y}$ coordinate around the cylinder. The dashed central line is a reference showing the central axis of the tube. The arrows show the sense of the motion of the bubbles. Fluid draining into and through the foam moves preferably in the vertical direction, due to gravity.

2 Experimental procedure and observations

A column of foam was created by blowing nitrogen gas through a syringe needle into a solution of the commercial detergent Fairy Liquid, and collecting the bubbles in a glass tube. We used glass tubes with diameter $d =$ 2.05 cm and length 35.5 cm. The foams were monodisperse with bubble radii of $r_b =$ 1.55 mm.

A forced drainage experiment was performed by adding the same surfactant solution at the top using a Watson-Marlow 505S peristaltic pump, which allows increments of 0.03 ml/s in flow rate Q. The result was observed for a range of tilt angles up to $25°$.
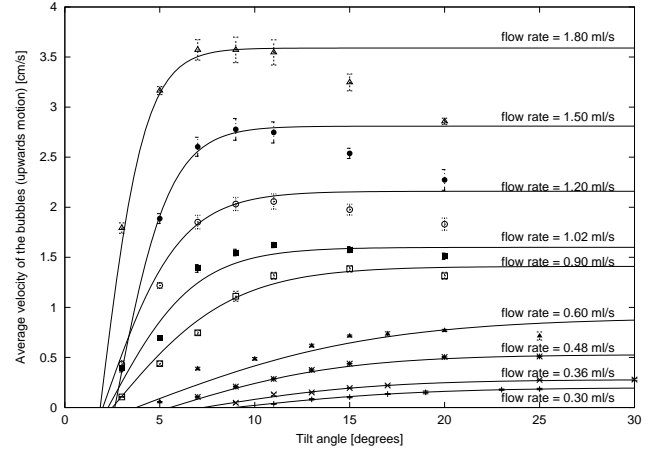
The bubble motion that is observed is the simple convective roll indicated in figure 1. The downward-travelling side
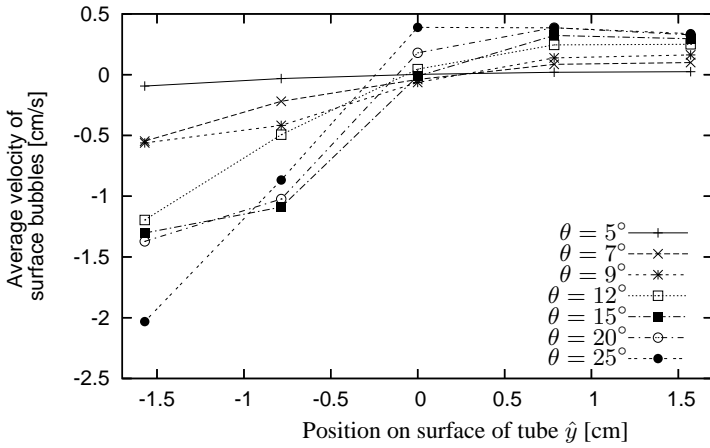
Fig. 2. The velocity of the surface bubbles (each point represents an average of six measurements) in different positions around the surface of the tube, with $\hat{y} = -\frac{1}{2}\pi$ cm corresponding to the lower boundary of the tube. The input flow rate was fixed at $Q = 0.408$ ml/s. Bubbles at $\hat{y} = 0$ start to move upwards at angles above $12°$. The width of the wet region decreases when the tube is tilted, while the speed of bubbles above the centreline is fairly constant at each angle, which is consistent with the plug flow observed visually. Error bars have been omitted for clarity.

Fig. 3. The upward velocity of bubbles in the dry foam in relation to the tilt angle θ. The data are fitted to the function $v(\theta) = v_{\lim} \tanh((\theta - \theta_c)/\theta_0)$ and each curve labeled with the fixed flow rate at which the data were taken. For small angles, an increase in θ leads to an increase in velocity. At higher angles, we see that for low flow rates the velocity reaches a plateau, $v_{\lim}$, while for higher flow rates, the bubbles slow down slightly. In fitting the data to the ansatz given in (1), we ignore these points, which only affects flow rates higher than about 1 ml/s.

is visibly "wetter", that is, of higher liquid fraction, and travels with velocities that are of the order of 1cm/s. The upward-travelling side has a lower velocity of the order of a few mm/s. Various measurements of surface bubble velocities were made, confirming the visual observation that the dry foam undergoes plug flow, while the wet foam is continuously sheared (figure 2).

This type of motion has also been observed in the case of the vertical tube, but in recent work we have also found a cylindrically symmetric form of convection in which all the surface bubbles move downwards together and the return motion is in the centre of the tube [7].

For the present case of the tilted tube, we observe only the simple roll described above, and for further analysis we characterise it by the velocity of plug flow on the dry, upper, side.

Figure 3 presents data for a range of flow rates. It is evident that there is in each case a critical angle θ_c below which there is no convection. The velocity of convection increases rapidly when the angle is increased from this critical value, and eventually saturates. Of course this description does not apply in full at higher flow rates, for which the critical angle goes to zero.

The three parameter fitting function

$$v(\theta) = v_{\lim} \tanh((\theta - \theta_c)/\theta_0) \tag{1}$$
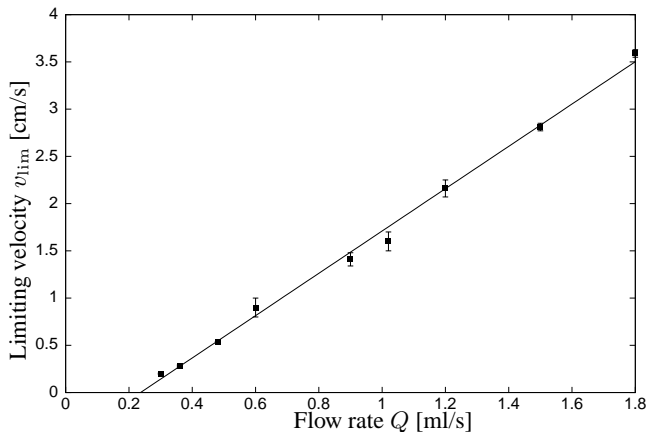
Fig. 4. The limit velocity v_{lim} reached by the convective roll in a tilted tube varies linearly with flow rate. Extracted from the data of figure 3.

Fig. 5. The motion of bubbles in the tilted tube begins, for given flow rate Q, when the angle of tilt is increased beyond a critical value θ_c. The solid line is a fit to the form given in (17), $\theta_c \propto Q^{-3/4}$, with a coefficient of proportionality of 3.17 ± 0.17. The inset shows the data on log scales.
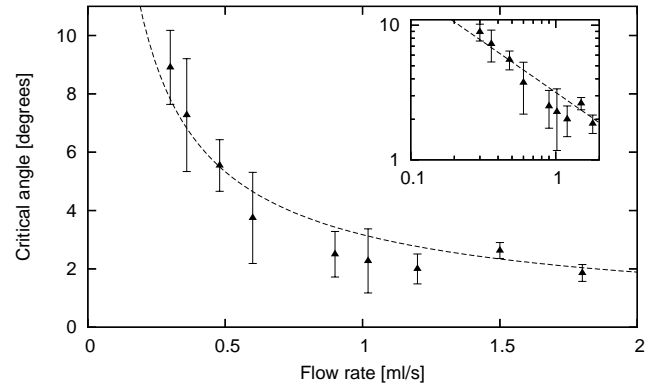
was found to be a convenient representation of the data: we make no claim for this particular analytic form, although the implied initial linear increase of $v(\theta)$ seems reasonable.

In this way we reduce the data to two key dependencies, those of limiting velocity v_{lim} and critical angle θ_c on flow rate Q. These are shown in figures 4 and 5. The limiting velocity is linear in flow rate, to within a good approximation. The critical angle shows a roughly inverse relation with flow rate: the curve included in figure 5 is fitted using

$$\theta_c = const. \times Q^{-3/4}, \tag{2}$$

as suggested by the theory which follows. The fit appears to be satisfactory.

It must fail in the limit of high Q, since there is spontaneous convection for $\theta = 0$ at some critical value of Q, as previously observed.

3 Theoretical analysis

3.1 Liquid fraction profile

Drainage in a vertical tube at low flow rates entails a distribution of liquid fraction which is cylindrically symmetric about the tube axis. In the elementary theory it is treated as a constant. This symmetry is broken by tilting the tube (figure 1). In the absence of convective motion, and even in this case over most of the length of the tube, there is no *transverse* flow of liquid. A transverse variation of liquid fraction is produced by the relevant component of gravity, $g \sin \theta$. This is the same variation that is familiar in the vertical profile of static equilibrium in a vertical tube [12] as follows. (This is a special case of the standard drainage theory.) For the surfactant used in these experiments, the so-called channel-dominated drainage equation is an appropriate model of the drainage process.

Using the variables defined in the Appendix, the cross-sectional area of the Plateau border A obeys

$$\rho g \sin \theta \, A^2 + \frac{C\gamma}{2} \sqrt{A} \frac{\partial A}{\partial Y} = 0, \qquad (3)$$

where Y is as defined in figure 1. The solution is

$$A(Y) = \left[\frac{\rho g}{C\gamma} \, \sin \theta \, (Y - Y_0) \right]^{-2} \qquad (4)$$

where the constant Y_0 is as yet undetermined. The liquid fraction is then

$$\Phi_l(Y) = \frac{K_1}{\sin^2 \theta} \, (Y - Y_0)^{-2} \qquad (5)$$

with $K_1 = c_1 / V_b^{2/3} (C\gamma/\rho g)^2 \approx 8.96 \times 10^{-7} \mathrm{m}^2$. As is intuitively obvious, an excess of liquid gathers at the lower side of the tube. If this were to reach the maximum density of a foam (corresponding to the rigidity loss or melting transition) the present theory fails and this should be a consideration at high flow rates.

Again it appeals to intuition that this density variation induces the convective motion; an explicit argument will be given below. In order to do so it must overcome the yield stress of the foam, below which it behaves as an elastic solid [1]. It will be the competition between these two factors that will determine the critical angle θ_c.

At this point the cylindrical profile of the tube is a considerable complication, so we approximate it for the purposes of the present preliminary theory by substituting a square cross section, of side d, with two sides normal to the transverse direction. This enables us to write the liquid fraction (and hence the flow rate) as a function of Y only, and perform the necessary integrations analytically, to obtain the total (input) flow rate Q. That is, we integrate the flow rate in the Z direction,
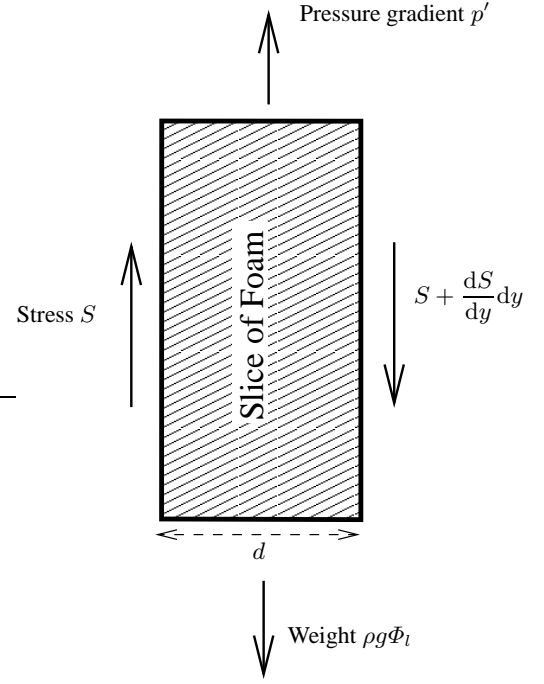
Fig. 6. The forces acting on a small element of the foam. The weight of the foam, $\rho g \Phi_l$, is balanced by the pressure gradient p' and the shear stresses on the wall.

$Q_Z = \rho g \cos \theta \, A^2/(3\eta_l f)$, across the width of the foam to get the total flow rate:

$$Q = \left(\frac{c_2 d}{r_b} \right)^2 \frac{1}{d} \int_{-\frac{1}{2}d}^{\frac{1}{2}d} Q_Z \mathrm{d}Y \qquad (6)$$

where the factor of $(c_2 d/r_b)^2$ represents the number of Plateau borders in any one cross-section of the tube with c_2 an unknown geometric constant. Thus

$$\begin{aligned} Q &= \left(\frac{c_2 d}{r_b} \right)^2 \frac{1}{d} \int_{-\frac{1}{2}d}^{\frac{1}{2}d} \mathrm{d}Y \, \frac{\rho g \cos \theta}{3\eta_l f} \left[\frac{C\gamma}{\rho g \, \sin \theta \, (Y - Y_0)} \right]^4 \\ &= c_2^2 K_2 \frac{\cos \theta}{\sin^4 \theta} \left[\frac{1}{(Y_0 - \frac{1}{2}d)^3} - \frac{1}{(Y_0 + \frac{1}{2}d)^3} \right] \qquad (7) \end{aligned}$$

to find $Y_0(Q)$ implicitly. The prefactor is $K_2 = d(C\gamma)^4/9\eta_l f(\rho g)^3 r_b^2 \approx 2.03 \times 10^{-4} \mathrm{ml}^2/\mathrm{s}$.

3.2 Stress profile

We now consider the forces acting on an element of the foam as shown in figure 6. We assume that the solution does not depend on vertical position Z (except for neglected end effects). In equilibrium, the weight of the foam is balanced by both the vertical pressure gradient p' and the gradient of shear stress on the tube wall. The condition on the stress S must therefore take the following form:

$$\frac{dS}{dy} = \rho g \Phi_l(y) + p'. \tag{8}$$

Here it is convenient to assume that the variation of liquid fraction $\Phi_l(y)$ is approximately linear and write $\Phi_l(y) = \Phi_l(0) + y \left.\frac{d\Phi_l}{dy}\right|_{y=0}$, where we have chosen $y = 0$ as the centre of the tube. Solving

$$\frac{dS}{dy} = \rho g \left(\Phi_l(0) + y \left.\frac{d\Phi_l}{dy}\right|_{y=0} \right) + p' \tag{9}$$

gives

$$S = (\rho g \Phi_l(0) + p') y + \frac{1}{2}\rho g y^2 \left.\frac{d\Phi_l}{dy}\right|_{y=0} + const. \tag{10}$$

The integration constant is found by imposing zero stress, $S = 0$, at $y = \pm\frac{1}{2}d$, corresponding to the assumption of no friction at the wall. This results in

$$S = \frac{\rho g}{2} \left.\frac{d\Phi_l}{dy}\right|_{y=0} \left(y^2 - \left(\frac{d}{2}\right)^2 \right). \tag{11}$$

The maximum stress amplitude is thus given by

$$\max|S| = \frac{1}{8}\rho g d^2 \left| \left.\frac{d\Phi_l}{dy}\right|_{y=0} \right|. \tag{12}$$

The liquid fraction Φ_l is directly proportional to the Plateau border area A, according to standard drainage theory, as in the Appendix. In the tilted tube, y is replaced with Y. $\Phi_l(0)$ is the liquid fraction at the centre of the foam. Therefore, as in (4),

$$\max|S| = K_3 \sin\theta \ (\Phi_l(0))^{3/2} \tag{13}$$

with $K_3 = 0.1(\rho g d)^2 V_b^{1/3}/(C\gamma) \approx 1086\text{N/m}^2$.

Now, consider the foam to have a yield stress S_0 which decreases with liquid fraction, $S_0 = S_{00}(1 - \Phi_l/\Phi_l^c)^2 \approx S_{00}(1 - \Phi_l(0)/\Phi_l^c)^2$ [13], where Φ_l^c is the critical liquid fraction of 36% at which the bubbles separate (the rigidity loss transition). S_{00} is approximately constant for small values of θ. At the onset of convection we have that

$$S_0 = \max|S| = K_3 \ \sin\theta_c \ (\Phi_l(0))^{3/2}. \tag{14}$$

For small angles $\theta_c \ll 1$, this results in

$$\theta_c \approx \frac{S_{00}}{K_3 \ (\Phi_l(0))^{3/2}} \left(1 - \frac{\Phi_l(0)}{\Phi_l^c} \right)^2. \tag{15}$$

The input flow rate (7) may be related to the liquid fraction in the centre of the foam column from (4), $\Phi_l(0) = K_1/(\sin\theta \ Y_0)^2$. So (15) gives an implicit relationship for the critical angle θ_c in terms of flow-rate Q.

To compare with the experimental data, we compute this to leading order. We expand the expression for Q to give

$$Q \approx \frac{c_2^2 K_2}{\sin^4\theta} \frac{3d}{Y_0^4} = \frac{3dc_2^2 K_2}{K_1^2} (\Phi_l(0))^2 \tag{16}$$

Therefore

$$\theta_c \approx \frac{S_{00}}{K_3} (\Phi_l(0))^{-3/2} \approx \frac{S_{00} c_2^{3/2} (3dK_2)^{3/4}}{K_3 K_1^{3/2}} Q^{-3/4}. \tag{17}$$

We choose a value of $S_{00} = 0.06\gamma/r_b$ [13], allowing us to fit the experimental data through the geometric constant c_2. We find a value of $c_2 = 3.96$, giving $\theta_c \approx 3.17Q^{-3/4}$. This is shown with the experimental data in figure 5. It seems extremely satisfactory within this range of data.

4 Outlook

We have presented experimental data for convective bubble motion in a tilted tube, together with a theoretical analysis for

the onset of the motion. While this is clearly a special case of convection in foams, it is nevertheless an important first step in being able to give a theoretical justification for the phenomenon.

An understanding of convection is necessary to be able to take steps to reduce or eliminate it. An industrially important example is that of the flotation process, in which ore is separated in a foam undergoing forced drainage [14, 15]. The ore is carried up, out of the gangue, with the foam, and then collected. Were the yield stress to become low enough in some part of the foam, either through increases in liquid fraction, flow rate or bubble size, then convective motion would cause the ore to be redistributed throughout the foam and the yield would drop.

The motion is, of course, caused by gravity, and prevents the study of uniformly wet foams on earth. The current generation of microgravity facilities (parabolic flights, rockets and the International Space Station) may therefore allow foam experiments and theory [16, 17] to move beyond the limit of low liquid fraction where we can demonstrate a fair level of understanding and a number of predictive guides for their behaviour.

Acknowledgements

References

1. D. Weaire and S. Hutzler. 1999 *The Physics of Foams*. Clarendon Press, Oxford.

2. D. Weaire, S. Hutzler, G. Verbist and E. Peters. 1997 A review of foam drainage. *Advances in Chemical Physics* **102**:315–374.

3. S.A. Koehler, S. Hilgenfeldt and H.A. Stone. 2000 A generalized view of foam drainage: Experiment and theory. *Langmuir* **16**:6327–6341.

4. S.A. Koehler, S. Hilgenfeldt and H.A. Stone. 2004 Foam drainage on the microscale: I. modeling flow through single plateau borders. *J. Coll. Interf. Sci.* **276**:420–438.

5. S. Hutzler, D. Weaire and R. Crawford. 1998 Convective instability in foam drainage. *Europhysics Lett.* **41**:461–465.

6. M.U. Vera, A. Saint-Jalmes and D.J. Durian. 2000 Instabilities in a liquid-fluidized bed of gas bubbles. *Phys. Rev. Lett.* **84**:3001–3004.

7. D. Weaire, S. Hutzler, S. Cox, N. Kern, M.D. Alonso and W. Drenckhan. 2003 The Fluid Dynamics of Foams. *J. Phys.: Condens. Matter* **15**:S65–S73.

8. S. Hutzler, D. Weaire and S. Shah. 2000 Bubble sorting in a foam under forced drainage. *Phil. Mag. Lett.* **80**:41–48.

9. A.E. Boycott. 1920 Sedimentation of blood corpuscles. *Nature* **104**:532–533.

10. E. Guyon, J.P. Hulin and L. Petit. 1991 *Hydrodynamique physique*. InterEditions, Editions du CNRS.

11. J. Duran and T. Mazozi. 1999 Granular Boycott effect: How to mix granulates. *Phys. Rev. E* **60**:6199–6201.

12. H.M. Princen and A.D. Kiss. 1987 Osmotic-pressure of foams and highly concentrated emulsions. 2. Determination from the variation in volume fraction with height in an equilibrated column. *Langmuir* **3**:36–41.

13. A. Saint-Jalmes and D.J. Durian. 1999 Vanishing elasticity for wet foams: Equivalence with emulsions and role of polydispersity. *J. Rheol.* **43**:1411–1422.

14. B.A. Wills. 1997 *Minerals Processing Technology: An Introduction to the Practical Aspects of Ore Treatment and Mineral Recovery*. Butterworth-Heinemann, Oxford. 6th edition.

15. S.J. Neethling and J.J. Cilliers. 1998 The effect of weir angle on bubble motion in a flotation froth: visual modelling and verification. *Minerals Engng.* **11**:1035–1046.

16. S. Marze, A. Saint-Jalmes, D. Langevin, S. Cox and D. Weaire 2005 Aqueous foam experiments in the Maxus 6 rocket: towards the development of an ISS module. In *Proc. 17th ESA Symposium on European Rocket and Balloon Programmes and Related Research* **SP-590**. ESA, The Netherlands.

17. S.J. Cox and G. Verbist. 2003 Liquid flow in foams under microgravity. *Microgravity Science and Technology* **XIV/4**:45–52.

18. G. Verbist, D. Weaire and A.M. Kraynik. 1996 The foam drainage equation. *J. Phys.: Condensed Matter* **8**:3715–3731.

19. S.J. Cox, D. Weaire, S. Hutzler, J. Murphy, R. Phelan and G. Verbist. 2000 Applications and Generalizations of the Foam Drainage Equation. *Proc. R. Soc. Lond. A* **456**:2441–2464.

Appendix

Our theoretical model uses the channel-dominated foam drainage equation for rigid interfaces, appropriate to the detergent used in the experiments [1, 2, 18]. It relates the cross-sectional area of the Plateau borders A to their position (y, z) (with z vertically downwards and y horizontal) in the foam at time t. The balance of forces is between gravity, viscous drag on the walls of the Plateau borders, and the pressure gradient between regions of different liquid fraction.

Liquid density, viscosity and surface tension are denoted by ρ, η_l and γ respectively. The acceleration due to gravity is g and the bubble volume is V_b. The liquid fraction of the foam is directly proportional to the area A [1]:

$$\Phi_l = \frac{c_1}{V_b^{2/3}} A. \tag{18}$$

The constant of proportionality c_1 is, although dependent upon the precise structure of the foam, close to 5.35, and we shall use that value here.

In its two-dimensional form [19], the drainage equation can be written

$$\frac{\partial A}{\partial t} + \nabla.\underline{Q} = 0 \tag{19}$$

where the flow rate $\underline{Q} = (Q_y, Q_z)$ is

$$\underline{Q} = \frac{1}{3\eta_l f}\left(-\frac{\gamma C}{2}\sqrt{A}\frac{\partial A}{\partial y},\ \rho g A^2 - \frac{\gamma C}{2}\sqrt{A}\frac{\partial A}{\partial z}\right) \tag{20}$$

where the geometric constants are $f \approx 50$ and $C^2 = 0.16$.

For a tube of foam that is tilted at an angle θ, we define Z and Y to be the co-ordinates along and perpendicular to the axis of the tube:

$$Z = z\cos\theta + y\sin\theta \quad \text{and} \quad Y = -z\sin\theta + y\cos\theta. \tag{21}$$

For this tilted geometry the flow rates in (20) are written $\underline{Q} = (Q_Y, Q_Z)$, where

$$\underline{Q} = \frac{1}{3\eta_l f} \left(-\rho g A^2 \sin\theta - \frac{\gamma C}{2}\sqrt{A}\frac{\partial A}{\partial Y}, \right.$$
$$\left. \rho g A^2 \cos\theta - \frac{\gamma C}{2}\sqrt{A}\frac{\partial A}{\partial Z} \right) \qquad (22)$$

At constant flow rate (steady drainage) throughout the foam, the time derivative of A may be neglected, in which case (19) represents the balance of flow rates in each of the two directions. The boundary conditions on these flow rates are that in the Y direction the flow rate is zero at $Y = \pm\frac{1}{2}d$ (the tube walls) and in the Z direction the flow rate of liquid at top and bottom is equal to the input flow rate.

Since there is no flow in the Y direction at the sides of the foam, there can be no flow in this direction anywhere. Thus all liquid motion is in the Z direction, parallel to the tube walls, and $A = A(Y)$ satisfies eqn. (3).

We take typical values of the material parameters throughout: $\rho = 1000\text{kg/m}^3$, $g = 9.8\text{m/s}^2$, $\gamma = 0.025\text{N/m}$ and $\eta_l = 0.001\text{Ns/m}^2$.